BIOCHEMISTRY
including biophysical chemistry & molecular biology

Article

pubs.acs.org/biochemistry

Structural Analysis of Activated SgrAI–DNA Oligomers Using Ion Mobility Mass Spectrometry

Xin Ma, Santosh Shah, Mowei Zhou, Chad K. Park, Vicki H. Wysocki,* and Nancy C. Horton*

Department of Chemistry and Biochemistry, University of Arizona, Tucson, Arizona 85721, United States

Supporting Information

ABSTRACT: SgrAI is a type IIF restriction endonuclease that cuts an unusually long recognition sequence and exhibits self-modulation of DNA cleavage activity and sequence specificity. Previous studies have shown that SgrAI forms large oligomers when bound to particular DNA sequences and under the same conditions where SgrAI exhibits accelerated DNA cleavage kinetics. However, the detailed structure and stoichiometry of the SgrAI–DNA complex as well as the basic building block of the oligomers have not been fully characterized. Ion mobility mass spectrometry (IM-MS) was employed to analyze SgrAI–DNA complexes and show that the basic building block of the oligomers is the DNA-bound SgrAI dimer (DBD) with one SgrAI dimer bound to two precleaved duplex DNA molecules each containing one-half of the SgrAI primary recognition sequence. The oligomers contain variable numbers of DBDs with as many as 19 DBDs. Observation of the large oligomers shows that nanoelectrospray ionization (nano-ESI) can preserve the proposed activated form of an enzyme. Finally, the collision cross section of the SgrAI–DNA oligomers measured by IM-MS was found to have a linear relationship with the number of DBDs in each oligomer, suggesting a regular, repeating structure.

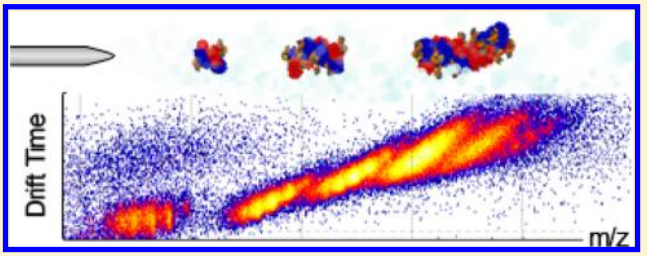

Restriction endonucleases (ENases) are bacterial enzymes that bind to specific DNA sequences (recognition sites) in duplex DNA and cleave at or near this sequence.[1−4] Most type II ENases recognize and cleave 4–6 bp sites. ENases with long and specific recognition sites are useful in genomic technology because of the lower frequency of occurrence of the longer sequences producing larger DNA fragments.[5,6] SgrAI is a type IIF ENase from *Streptomyces griseus* that recognizes an 8 bp DNA sequence, 5′ CR|CCGGYG 3′ (where R = A or G, Y = C or T, and | indicates the site of cleavage), known as the cognate or primary site.[7] SgrAI also cleaves at secondary sites, 5′ CR|CCGGY(A,C,T) 3′ and 5′ CR|CCGGGG 3′, under particular reaction conditions. SgrAI cleaves plasmids with two copies of the primary site faster than plasmids with only one copy. In addition, when both primary and secondary sites are on the same plasmid, SgrAI cleaves both sites, although cleavage of the secondary site is slower (approximately 26-fold) than that of the primary site. However, in the absence of the primary site, the cleavage rate of the secondary site is significantly slower (200-fold).[8−10] It has also been shown that the precleaved primary site DNA sequence will stimulate the cleavage of primary and secondary sites by SgrAI. Such a self-activation with expansion of sequence specificity is unusual in type II ENases.[8,9,11]

The X-ray crystallographic structures of the homologous (as evidenced by their common core fold and similar DNA recognition sequences) type IIF ENases SfiI, NgoMIV, and Cfr10I show homotetramers composed of two dimers in a tail-to-tail orientation.[12−14] Two duplex DNA molecules containing the recognition sequence bind to opposite sides of the tetramer.[12−16] However, SgrAI is a dimer in solution without DNA.[6,11] Both Mg^{2+} and Ca^{2+} stimulate DNA binding by most ENases, with Mg^{2+} conferring cleavage activity and Ca^{2+} inhibiting DNA cleavage but maintaining site specific DNA binding activity.[17−23] SgrAI has been shown to form large and heterogeneous species in the presence of primary site DNA containing sufficient flanking sequences, and under the same conditions where activation of DNA cleavage by SgrAI occurs.[6,11] Native gel electrophoresis and analytical ultracentrifugation show that the oligomer is heterogeneous and composed of possibly 4–12 DNA-bound SgrAI dimers (DBDs). However, the exact size, stoichiometry, and basic building block of these species (inferred as DBD^6) have not been measured directly.

Structural information about noncovalent protein complexes is important in understanding the mechanism of protein function.[24−29] X-ray crystallography and nuclear magnetic resonance (NMR) can provide high-resolution structural information; however, these techniques require a large amount of pure and homogeneous protein. Because the SgrAI–DNA oligomers are heterogeneous in size based on analytical ultracentrifugation results,[6] analysis via X-ray crystallography is challenging. Nanoelectrospray ionization (nano-ESI) mass spectrometry (MS) is widely used to determine stoichiometry, and with specialized tandem MS (MS/MS) and IM experiments, the spatial organization, or topology, of supramolecular complexes in the gas phase can also be investigated.[29]

Received: September 27, 2012
Revised: June 4, 2013
Published: June 6, 2013

Considerable evidence supports the idea that protein assemblies remain intact and folded in vacuum.[24−30] However, nano-ESI-MS cannot provide atomic-level information for protein complexes.

Ion mobility mass spectrometry (IM-MS) has been coupled with nano-ESI to gain geometric information about protein complexes.[24] The collision cross section (CCS) includes information about the physical size and shape of the ion. Under the acceleration of electric fields, ions with larger CCSs and lower charge states migrate slower in the drift tube filled with bath gas, analogous to the concept of electrophoresis. Therefore, the drift times of different ions reflect differences in the charge state and CCS.[31,32] Protocols have been developed to calculate the ion bath gas CCS based on X-ray crystallograpic or NMR structures. The Jarrold group has developed an open source software program, MOBCAL, to calculate helium-based CCSs of biological molecules with three approaches:[33,34] projection approximation (PA), exact hard sphere scattering (EHSS), and the trajectory method (TM).[35,36] PA determines the CCS by averaging all possible geometric projection areas. The calculation is simpler than the other two methods because it does not consider scattering processes and long-range interactions between the ions and the bath gas. Consequently, PA underestimates the CCSs.[37,38] EHSS calculates the CCS by averaging the momentum transfer cross section that is related to the scattering angle over the relative velocity and the collision geometry. However, EHSS ignores long-range interactions.[33,34,38] The TM takes into account scattering, long-range interactions, and the effect of multiple collisions, and it is considered to be the most reliable and accurate CCS calculation approach. In this method, interatomic potentials are defined and then the trajectories are calculated within the potentials to obtain the scattering angles. The disadvantage of the TM is that the calculation is the most computationally intense of the three methods.[36,39] PA and EHSS are widely used for large molecule CCS calculations,[40−45] but the deviation between PA and EHSS can be as large as 20% for some geometries with grossly concave surfaces.[33] In the study presented here, an empirical method, named scaled PA and developed by the Robinson group, was used, because the calculated CCSs using scaled PA agree with the experimentally measured CCSs.[46,47]

Different charge states of the same protein usually have different CCSs. In most cases, as the number of charges increases, the CCS increases. This is believed to be due to unfolding or other expansion of the protein structure caused by repulsion between the greater number of charges, leading to a larger CCS.[35,48,49] However, the situation has been found to be different for some complexes. The TRAP 11-mer ring, for example, collapses (CCS decreases) with an increasing number of charges.[40] Generally, the lower charge states of proteins are used to calculate CCSs because they are more likely to be those of the native state.[35,48,49]

In this work, SgrAI−DNA complexes were analyzed by IM-MS under nativelike conditions. SgrAI−DNA oligomers of different sizes were observed, and their masses indicate that the DBD is the basic building block of these oligomers, with one SgrAI dimer bound to two copies of the precleaved SgrAI primary recognition site (PC DNA) in each DBD. The experimentally determined CCSs of the SgrAI−DNA oligomers were found to have a linear relationship with the number of DBDs per oligomer, suggesting a regular, repeating structure in the oligomers. Via comparison of the CCSs of the SgrAI dimer bound to DNA of different lengths, the conformation of the DNA in the unoligomerized DBD IM-MS is proposed.

MATERIALS AND METHODS

Protein Preparation. Wild-type SgrAI ENase was expressed and purified as described previously[6,50] and estimated to be 99% pure by Coomassie-stained sodium dodecyl sulfate−polyacrylamide gel electrophoresis. Before analysis, the SgrAI was dialyzed into a buffer containing 300 mM ammonium acetate and 1 mM dithiothreitol (DTT) using a Slide-A-Lyzer MINI dialysis device, with a 3.5K molecular weight cutoff (Thermo Fisher Scientific, Rockford, IL) at 4 °C. The final concentration of SgrAI was measured on the basis of the absorbance at 280 nm with a Thermo Scientific (Wilmington, DE) NanoDrop 2000 microvolume UV−visible spectrophotometer, and the extinction coefficient of SgrAI was derived from the protein sequence.[51]

DNA Preparation. The oligonucleotides were made synthetically and purified using C18 reverse phase high-performance liquid chromatography by Sigma-Aldrich (St. Louis, MO). The concentration of each single strand was then measured spectrophotometrically with extinction coefficients calculated from standard values for the nucleotides.[52] DNA samples were annealed and aliquoted into small amounts, flash-frozen in liquid nitrogen, and stored at −80 °C. Each aliquot was used only once after being removed from the freezer.[6,50] The sequences of the 40 bp secondary site (40-2) DNA, PC DNA, and PC minus 9 flanking bp (PC-9) DNA are shown below, with recognition sites colored red:

40-2 (2° site)	5'-GATGCGTGGGTCTTCACACCGGGGTGAAGACCCACGCATC-3' 3'-CTACGCACCCAGAAGTGTGGCCCCACTTCTGGGTGCGTAG-5'
PC	5'-GATGCGTGGGTCTTCACA-3' 3'-CTACGCACCCAGAAGTGTGGCC-5'
PC-9	5'-GTCTTCACA-3' 3'-CAGAAGTGTGGCC-P5'

IM-MS. SgrAI (10−12 μM) and DNA were placed in a buffer with 100 mM ammonium acetate, 5 mM calcium tartrate, and 1 mM DTT, which gave SgrAI dimer:DNA mole ratios of 1:1 to 1:4. Nano-ESI-MS was used to analyze the SgrAI−DNA solution on a Synapt G2 HDMS instrument (Waters MS Technologies, Manchester, U.K.) as described in the literature.[53−56] Briefly, each sample was loaded into a tapered glass capillary pulled in-house using a Sutter Instruments (Novato, CA) P-97 micropipet puller. A platinum wire was inserted into the nontapered end of the capillary, and a voltage of 1.1−1.6 kV was applied until optimal ion transmission and protein desolvation were achieved. The cone voltage was optimized at 50 V, and the ion source temperature was ∼30 °C to minimize denaturation of protein or DNA. Pressure in the source region was increased to ∼7 mbar by partially restricting the vacuum line to the rotary pump to optimize ion collisional cooling and transmission.

All samples were analyzed with argon as the collision gas and nitrogen as the ion mobility gas. The pressure of argon in the transfer ion guide was 3.0×10^{-2} mbar, and the pressure of argon in the trap was 4.6×10^{-2} mbar. Collision-induced dissociation (CID) was performed over a range of collision voltages in the trap collision cell, with the "quadrupole profile" set to 10000 to transmit ions with m/z values from 8000 to 30000 efficiently. The flow rate of the helium cell was 180 mL/min. The pressure of nitrogen in the ion mobility cell was 3.2 mbar. The ion mobility spectrometry (IMS) wave height and velocity were optimized at 16.0 V and 200 ms^{-1}, respectively.

dx.doi.org/10.1021/bi3013214 | Biochemistry 2013, 52, 4373−4381

The time-of-flight (TOF) analyzer pressure was 9.0×10^{-7} mbar. The IM-MS conditions were optimized on the basis of the literature and research group experience with large complexes.[41]

Calibration of the CCS was performed as described.[35] Native serum amyloid P (EMD Millipore Corp., Chicago, IL) pentamer and decamer and concanavalin A (Sigma-Aldrich) tetramer were used as standard proteins to create a CCS calibration curve because their sizes are similar to those of the analytes. All mass spectra were analyzed with MassLynx version 4.1, and all mobiligrams were visualized using DriftScope version 2.1 provided by Waters MS Technologies.

CCS Calculation and Model Building. Theoretical CCSs were calculated using the PA and EHSS methods in MOBCAL using models prepared from X-ray crystallographic structures.[41] Scaled PA was used to calculate the theoretical CCSs.[46,47] The DBD models with different DNA conformations were prepared manually using the PyMOL Molecular Graphics System, version 1.5.0.4 (Schrödinger, LLC).[57] B-Form DNA was manually added to the ends of the DNA in the X-ray crystal structure of SgrAI bound to cleaved primary site DNA (Protein Data Bank entry 3MQY[58]). Bends in the modeled DNA were introduced manually using PyMOL, taking care to maintain proper bond lengths and angles. Computations of CCSs with MOBCAL were performed on a 2.83 GHz quad-core Xeon SGI (Fremont, CA) Altix ICE 8200 server at the University of Arizona.

RESULTS

Spectra of SgrAI Alone and with 40-2 and PC DNA. Nano-ESI-MS was used to detect species in solutions of SgrAI alone (Figure 1A) and SgrAI with DNA (Figure 1B,C). The spectrum of SgrAI without DNA (Figure 1A) showed mostly SgrAI dimer, as expected,[6,11] with a small amount of the total signal corresponding to SgrAI tetramer. Three different DNA constructs were also examined for their effects on oligomerization of SgrAI. The sequence 40-2 is a 40 bp duplex DNA containing a secondary site SgrAI recognition sequence (Materials and Methods). Secondary site sequences differ from primary site sequences by 1 bp and are cleaved slowly by SgrAI in the absence of primary site sequences.[6,8,9] SgrAI presented as largely dimeric, bound to one copy of 40-2, in the spectrum (Figure 1B), with some SgrAI tetramer bound to two copies of 40-2, and a very small amount of hexamer bound to three copies of 40-2 (Figure 1B). Next, the primary site sequence PC DNA, which mimics the product of cleavage by SgrAI, was analyzed (Figure 1C). The spectrum of SgrAI with PC DNA, at an SgrAI dimer:PC DNA molar ratio of 1:2, shows a dimer of SgrAI bound to two copies of PC DNA, as well as a significant amount of larger species, including SgrAI tetramer−4PC DNA and SgrAI hexamer−6PC DNA forms. In addition, unresolved species are found at m/z 9000−13000 (Figure 1C). The masses of all of the identifiable species are consistent with two copies of PC DNA binding per SgrAI dimer.

The effect of varying the molar ratio of SgrAI dimer to PC DNA was examined using nano-ESI mass spectrometry (Figure S1 of the Supporting Information). At a molar ratio of 1:1, SgrAI dimer−2PC DNA (1 × DBD) and SgrAI tetramer−2PC DNA (2 × DBD) complexes were observed (Figure S1A and Table S1 of the Supporting Information). Some species with higher m/z values were also found; however, their abundances were relatively small. A large unresolved species at m/z 4000−5000 that overlaps with the peaks for the DBD occurs [SgrAI dimer bound to two copies of PC DNA (Figure S1B−D of the Supporting Information)]. At a molar ratio of 1:2, SgrAI dimer−2PC DNA (1 × DBD), SgrAI tetramer−4PC DNA (2 × DBD), and SgrAI hexamer−6PC DNA (3 × DBD) complexes are observed (Figure 1C and Figure S1B of the Supporting Information). In addition, high-m/z species are also observed but with unresolvable peaks (Figure 1C and Figure S1B and Table S1 of the Supporting Information). At the two higher ratios [1:2.6 and 1:4 (Figure S1C,D of the Supporting Information)], the SgrAI hexamer−6PC DNA species is no longer resolvable, and the relative intensities of species above m/z 8000 decrease.

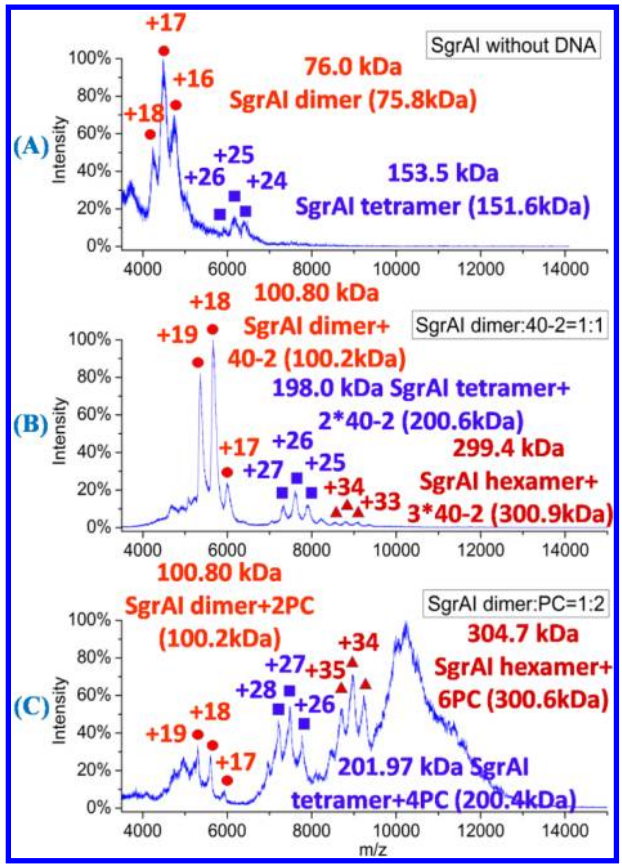

Figure 1. Spectra of SgrAI and SgrAI with different types of DNA. (A) SgrAI without DNA. Peaks corresponding to the SgrAI dimer (red circles) and SgrAI tetramer (purple squares) are visible. (B) SgrAI with 40-2 DNA (molar ratio of 1:1). Peaks corresponding to the SgrAI dimer bound to one duplex of 40-2 DNA (red circles), SgrAI tetramer bound to two 40-2 duplexes (purple squares), and SgrAI hexamer bound to three 40-2 duplexes (red triangles) are visible. (C) SgrAI with PC DNA (molar ratio of 1:2). Peaks corresponding to the SgrAI dimer bound to two PC DNA duplexes (red circles), SgrAI tetramer bound to four PC DNA duplexes (purple squares), and SgrAI hexamer bound to six PC DNA duplexes (red triangles) are visible, along with a large unresolved peak (m/z 900−1200). The theoretical masses are listed in parentheses.

Collision-Induced Dissociation (CID) To Resolve Species. CID was used to attempt to resolve peaks from the broad features in some spectra. Figure S2 of the Supporting Information shows the effect of increasing collision voltage in the MS/MS quadrupole-selected high m/z range in radio-frequency profile mode, m/z 8000−30000 selected, of the 1:2.6 molar ratio mixture of SgrAI dimer with PC DNA. Low-energy CID may result in larger SgrAI−DNA oligomers dissociating to

dx.doi.org/10.1021/bi3013214 | Biochemistry 2013, 52, 4373−4381

smaller species that can then be distinguished. In the experiment, the "quadrupole profile" was set to transport ions with m/z values from 8000 to 30000 efficiently. The ions were then dissociated by CID at different collision energies. With a low collision voltage (4 V), no obvious peaks were observed in the spectrum of the SgrAI–PC DNA complex with a molar ratio of 1:2.6 (Figure S2A of the Supporting Information). At a collision voltage of >30 V, some peaks of the SgrAI hexamer–6PC DNA complex (3 × DBD) (Table S2 of the Supporting Information) appeared at m/z 8400 and their relative abundance increased as well (Figure S2B of the Supporting Information). In addition, the magnitude of the broad peak at m/z 10700 decreased. At collision voltages of 50 and 70 V, the spectrum showed no obvious additional changes (Figure S2C,D of the Supporting Information). Thus, the peaks corresponding to the SgrAI hexamer–6PC DNA complex can be clearly resolved at 50 V (Figure S2C and Table S2 of the Supporting Information), are nearly resolved at 30 V (Figure S2B of the Supporting Information), and remain similar at 70 V (Figure S2D of the Supporting Information) and 50 V (Figure S2C of the Supporting Information). The broad peak at m/z 9000–10000 remained unresolvable even at 70 V (Figure S2D of the Supporting Information).

Low-energy CID was also used to investigate unresolved features of the spectrum of SgrAI with PC-9 DNA (Figure S3 and Table S3 of the Supporting Information). PC-9 has fewer flanking base pairs (7 bp) than PC DNA (16 bp). The length of DNA flanking the recognition sequence has been shown to influence activation and oligomerization of SgrAI.[51] The spectrum of SgrAI with PC-9 (at a 1:2 SgrAI dimer:PC DNA ratio) with CID of 4 V shows three broad, unresolved peaks (Figure S3A of the Supporting Information). At 30 V, peaks corresponding to SgrAI dimer–2PC-9 DNA and SgrAI tetramer–4PC-9 DNA complexes are resolvable (Figure S3B of the Supporting Information). The magnitudes of the features in general appear to be diminished with CID, and the feature at m/z 12000–14000 nearly disappears altogether.

Ion Mobility Mass Spectrometry (IM-MS) To Resolve Species. IM-MS was utilized to resolve species with overlapping m/z values (Figure 1) in a 1:2 molar ratio mixture of SgrAI dimer with PC DNA. Species are separated by drift time as well as m/z, and drift time varies with CCSs and charge states. Six clusters can be discerned, labeled I–VI (Figure 2A). Clusters I–III contain peaks in m/z values corresponding to SgrAI dimer–2PC DNA, SgrAI tetramer–4PC DNA, and SgrAI hexamer–6PC DNA complexes, respectively. No interpretable m/z peaks are immediately discernible in clusters IV and V. However, close inspection of cluster VI (Figure 1B,C) shows peaks that appear to correspond to the SgrAI dodecamer–12PC DNA complex. Species in clusters IV and V were revealed using IM-MS of a 1:2.6 mixture of SgrAI dimer and PC DNA (Figures S4–S8 of the Supporting Information) and region selection. The highest-intensity region of cluster IV (Figures S4B and S7A–C of the Supporting Information) showed m/z peaks (Figures S4C and S6 of the Supporting Information) corresponding to the SgrAI eicosamer–20PC DNA complex, and the highest-intensity region of cluster V (Figures S5B and S7D,E of the Supporting Information) revealed m/z peaks (Figures S5C and S7 of the Supporting Information) corresponding to the SgrAI 38mer–38PC DNA complex. The identified peaks are reproducible (Figures S6 and S7 of the Supporting Information). Because the highest-intensity regions of the IM-MS spectra are difficult to discern in the spectral plots with log scales (Figures S4B and S5B of the Supporting Information), Figure S8 of the Supporting Information shows the plots on log, square root, and linear scales. The widths of the identified m/z peaks are narrower, relative to those of the smaller oligomers (Figure 1), because of region selection (see Figures S9 and S10 of the Supporting Information).

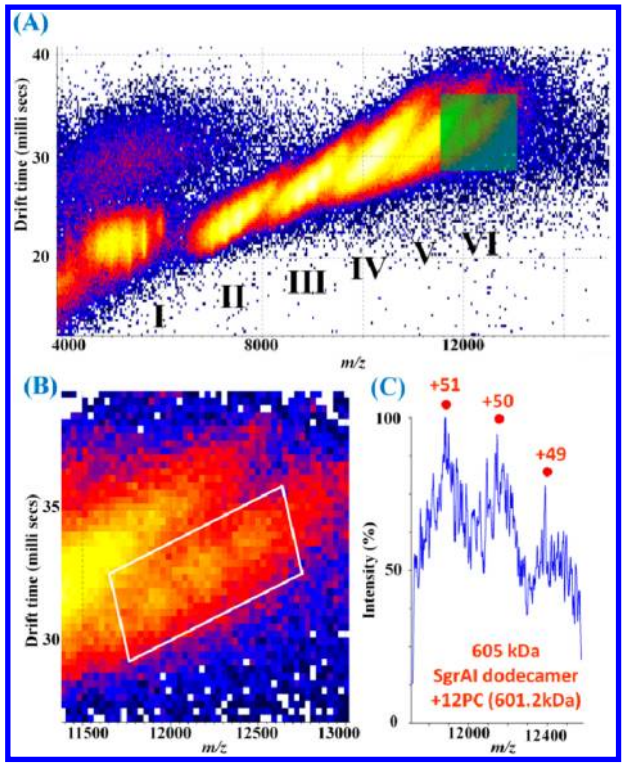

Figure 2. Mobiligram of the SgrAI dimer–PC DNA complex at a molar ratio of 1:2. (A) Six distinct regions are visible (I–VI). Regions I–III correspond to SgrAI dimer–2PC DNA, SgrAI tetramer–4PC DNA, and SgrAI hexamer–6PC DNA complexes, respectively. Regions IV–VI overlap in the mass spectrum (Figure 1C) but are distinct regions separated by drift time in IMS. (B) Enlargement of the green boxed region in panel A. (C) Spectrum extracted from the region in the white boxed region in panel B with peaks corresponding to the SgrAI dodecamer–12PC DNA complex. These peaks can be resolved only after IMS, which separates species that otherwise overlap in the mass spectrum.

From IM-MS, the CCSs were measured for each of the identified SgrAI–PC DNA species (Figure 3 and Table S4 of the Supporting Information). The CCS of the lowest discernible charge state of each oligomer was used to represent the CCS of the oligomer. A linear relationship was found between the CCS and the number of SgrAI dimer–2PC DNA complexes (Figure 3).

Model Building and CCS Comparison. The IM-MS CCSs of the SgrAI dimer, the SgrAI dimer–2PC-9 DNA complex, the SgrAI dimer–40-2 DNA complex, and the SgrAI dimer–2PC DNA complex were compared with those calculated CCSs from models derived from X-ray crystal structures (Figure 4 and Table S5 of the Supporting Information). The charge state for all of these complexes is +17. The CCSs of SgrAI bound to 40-2 DNA and SgrAI bound to PC DNA (blue and purple triangles, respectively, in Figure 4B) were found by IM-MS to be approximately 11% larger than the CCS of SgrAI with PC-9 DNA (red circles in Figure 4B). In other words, the 18 bp of added flanking DNA (9 bp on either

dx.doi.org/10.1021/bi3013214 | Biochemistry 2013, 52, 4373–4381

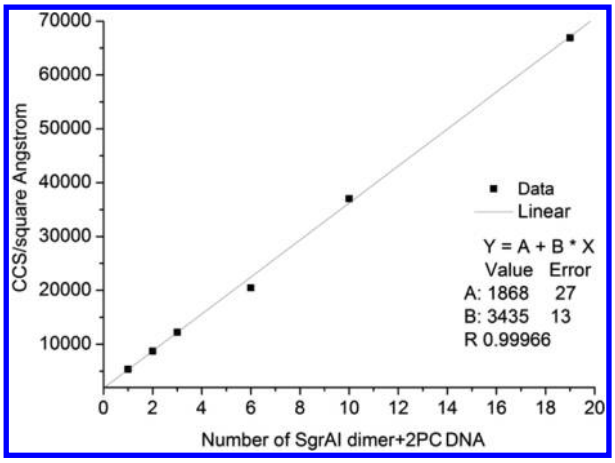

Figure 3. Linear relationship between experimental CCSs of SgrAI–PC DNA complexes and the number of DBDs.

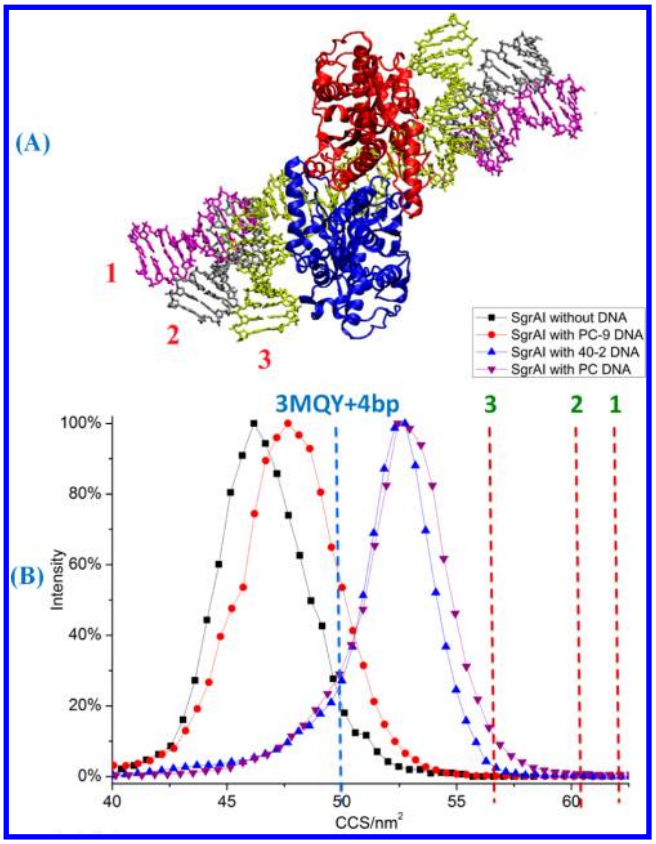

Figure 4. CCSs of SgrAI dimer with different DNA complexes. (A) Three different conformations of flanking DNA (labeled with different colors). Eleven base pairs of B-DNAs were added on both sides of X-ray crystallographic structure 3MQY as flanking DNA. Models with three different flanking DNA conformations were built. In the first model, the flanking DNA is modeled as straight B-form DNA elongated straightly outward into space. In the second model, the flanking DNA bends toward SgrAI by ~30° based on the first model. In the third model, the flanking DNA bends toward SgrAI by ~80°. (B) CCSs of experimental and modeled complexes: (black squares) SgrAI dimer without DNA, (red circles) SgrAI with PC-9 DNA, (blue triangles) SgrAI with 40-2 DNA, and (purple triangles) SgrAI with PC DNA complex. Dashed lines are calculated CCSs of 3MQY with 4 bp of modeled flanking DNA (two for each site of recognition sequence, blue dashed line) and calculated CCSs (red dashed lines) of models 1–3 (A).

side of the recognition sequence) present in the SgrAI dimer–2PC DNA complex relative to the SgrAI dimer–2PC-9 complex increases the CCS by ~11%.

The observed CCS was used to model the conformation of the DNA bound to SgrAI. The crystallographic structure of SgrAI bound to DNA, 3MQY, contains only 5 bp flanking the 8 bp SgrAI recognition site; therefore, the conformations of the additional 2 or 11 bp flanking this site that is present in PC-9 or both 40-2 and PC DNA, respectively, are not known. The flanking DNA influences formation of the large oligomers, and activation of DNA cleavage by SgrAI.[6,10] Models for the complexes of SgrAI bound to PC DNA and PC-9 DNA were prepared by the addition of flanking DNA (11 bp B-form on either side of the recognition sequence for PC DNA, 2 bp for PC-9 DNA) to the structure found in 3MQY.

The DNA conformation of the modeled flanking DNA in the model of SgrAI bound to PC DNA was varied giving rise to three different models (1–3, Figure 4A). In the first model, the flanking DNA extends with no bends (1 of Figure 4A). In the second model, the flanking DNA bends by 30° toward the SgrAI protein (2 of Figure 4A). In the third model, the flanking DNA bends as in the second model but by an additional 50° (80° total) (3 of Figure 4A). The CCSs were calculated for the model of the SgrAI dimer–2PC-9 DNA complex (3MQY with 4 bp DNA, blue dashed line, Figure 3B and Table S6 of the Supporting Information), and the three models of SgrAI dimer–2PC DNA complexes (1–3, red dashed lines, Figure 4B and Table S6 of the Supporting Information) using a linear combination method.[46,47]

DISCUSSION

The SgrAI Dimer–2PC DNA Complex (DBD) Is the Basic Building Block of the Oligomers. Previous studies have shown that SgrAI forms a homodimer in the absence of DNA.[6,11] Nano-ESI-MS was employed to analyze SgrAI without DNA to confirm that the native dimer can be preserved under the experimental conditions. The major species observed in the mass spectrum is the SgrAI dimer (Figure 1A and Table S1 of the Supporting Information). The SgrAI tetramer was also observed in a relatively smaller amount consistent with the dimer being the dominant species in solution at the given concentration. No remarkable larger oligomers were observed under these experimental conditions. The results show that the noncovalent interaction to form the SgrAI dimer can be preserved in nano-ESI-MS.

Secondary site DNA can bind to SgrAI but will not stimulate the DNA cleavage activity. A 40 bp DNA containing the secondary site sequence, 40-2 (Materials and Methods), was used to test the binding of secondary site DNA to SgrAI. SgrAI dimer with one 40-2 DNA, tetramer with two 40-2 DNA molecules, and a small amount of hexamer with three 40-2 DNA molecules were observed (Figure 1B and Table S1 of the Supporting Information). The relative ratio of the DNA-bound dimer to DNA-bound tetramer is similar to the ratio of dimer to tetramer in the absence of DNA (Figure 1A,B). No other obvious larger species were observed in this experiment. The mass spectra of SgrAI without DNA and SgrAI with 40-2 DNA reveal that 40-2 DNA does not stimulate formation of the larger oligomers, as found previously by other techniques.[6] In addition, DNA-bound SgrAI can be observed under these experimental conditions. The charge states of SgrAI without DNAare +16, +17, and +18, which are similar to those of 40-2 DNA-bound SgrAI (Figure 1A,B), suggesting that the negative

dx.doi.org/10.1021/bi3013214 | *Biochemistry* 2013, 52, 4373–4381

charges of 40-2 DNA were neutralized under the experimental conditions. The pK_a of the phosphodiester in DNA is ~3;[59] therefore, it is not expected to be protonated at pH 8.0. It is likely that cations such as calcium and ammonium are also attached, neutralizing the negative charge of the DNA. The number of these cations may vary in different experiments, so the theoretical masses do not include cation or neutral species attachment. As a result, most experimental masses (in parentheses in Figure 1) are larger than the theoretical masses by 1−2%. Furthermore, the attachment leads to peak broadening.[58]

To explore the influence of precleaved primary site DNA that can stimulate formation of the large oligomers,[6] different amounts of PC DNA were mixed with SgrAI, resulting in different molar ratios of SgrAI dimer to PC DNA. When the SgrAI dimer:PC DNA molar ratio was 1:1, only the SgrAI dimer−2PC DNA (1 × DBD) complex was observed, and not a complex with only one bound PC DNA. Two PC DNA molecules can form a DNA duplex structure that is similar to the uncleaved DNA substrate of the enzyme that binds tightly to the SgrAI dimer. If this interpretation is true, then the amount of SgrAI dimer−2PC DNA complex should increase when the SgrAI dimer:PC DNA ratio is 1:2.

When the SgrAI dimer:PC DNA ratio is 1:2, the relative amounts of large m/z species are greater (Figure S1B of the Supporting Information) than that in the 1:1 SgrAI dimer−PC DNA mixture (Figure S1A of the Supporting Information), suggesting that the 1:1 SgrAI dimer:PC DNA mixture molar ratio is not optimal for formation of the large m/z species. In the 1:2 molar ratio mixture, the observation of SgrAI tetramer−4PC DNA (2 × DBD) and SgrAI hexamer−6PC DNA (3 × DBD) complexes supports the DBD complex as the basic building block of the larger oligomeric species. The peaks at m/z 10000−13000 were not interpretable, possibly because of overlap from multiple species in the same m/z range derived from either neutral species attachment binding or oligomers with different masses. The complex of the SgrAI dimer with 40-2 DNA was found to contain mostly DBD (Figure 1B), consistent with previous work,[611] showing that the secondary site DNA does not stimulate SgrAI during oligomer formation. The large oligomers are found to occur only with DNA capable of activating the DNA cleavage activity of SgrAI; hence, they occur only when the enzyme is activated.[6] Thus, observation of the larger oligomers shows that nano-ESI can preserve not only native protein but also the activated form of an enzyme.

At SgrAI:PC DNA molar ratios of 1:2.6 and 1:4, the spectra are similar (Figure S1C,D of the Supporting Information); however, the total relative intensity of larger m/z species (above 8000) is reduced, and the SgrAI hexamer−6PC DNA species is no longer resolved. Both SgrAI dimer−2PC DNA (1 × DBD) and SgrAI tetramer−4PC DNA (2 × DBD) complexes are observed (Figure S1C,D and Table S1 of the Supporting Information). These results also support the 1:2 molar ratio as being optimal for forming larger SgrAI−DNA oligomers.

Low-energy CID was used to reduce the influence of nonspecific attachment of small molecules and/or salts to the protein and to investigate the composition of the SgrAI−DNA complexes, particularly in the unresolved peaks at m/z 8000−13000 in various spectra. The results suggest that CID either dissociated the larger m/z species to the SgrAI hexamer−6PC DNA complex (3 × DBD) or dissociated nonspecific attachment from this species, reducing its m/z complexity. If derived from the larger SgrAI−DNA oligomers, the results suggest that these large oligomers are less stable because they require a relatively low energy to dissociate to the SgrAI hexamer−6PC DNA (3 × DBD) complex. The SgrAI hexamer−6PC DNA (3 × DBD) complex was found to be stable at the highest collision voltage of the instrument and did not appear to dissociate into smaller species such as the SgrAI dimer−2PC DNA (1 × DBD) complex or the SgrAI tetramer−4PC DNA (2 × DBD) complex (Figure S1D of the Supporting Information). These results also show that when the concentration of PC DNA is equal to or higher than twice the SgrAI concentration, SgrAI−DNA oligomers can form.

CID was also used to distinguish peaks in the spectra of SgrAI bound to PC-9 DNA (Figure S3 of the Supporting Information). PC-9 DNA has fewer base pairs (7 bp) flanking the SgrAI recognition sequences than PC DNA [with 16 bp flanking (Materials and Methods)]. Previous studies have shown that a primary site with more flanking DNA binds tighter to SgrAI.[6] Also, sufficient flanking DNA is required for stimulation of the DNA cleavage activity of SgrAI.[6,10] At a SgrAI dimer:PC-9 DNA ratio of 1:2, no distinct peaks were observed and only unresolved broad features were present (Figure S3A of the Supporting Information). CID was then applied to dissociate nonspecific attachment of small molecules and/or salts or larger SgrAI−DNA oligomers overlapping in m/z values. Distinct peaks of SgrAI dimer−2PC-9 DNA (1 × DBD) and SgrAI tetramer−4PC-9 DNA (2 × DBD) complexes are observed at a CID of 30 V (Figure S3B and Table S3 of the Supporting Information), and much of the larger m/z species was diminished. The results show that large oligomers may form when PC-9 DNA is mixed with SgrAI, although the relative amount appears to be smaller than with PC DNA (Figure S2 of the Supporting Information). These results also show that the length of flanking DNA does not affect the ratio of the SgrAI dimer to PC DNA in the complexes.

Previous analytical ultracentrifugation results have shown that oligomers of DNA-bound SgrAI may contain as many as 12 DBDs.[6] The mass spectra of SgrAI−DNA complexes provide direct evidence that the DBD is the basic building block of these oligomers. However, the oligomers are heterogeneous, and their peaks overlap so the exact masses of these oligomers are still unclear from mass spectra alone, suggesting that ion mobility coupled to MS might help clarify the oligomeric states.

Linear Relationship between CCSs and the Number of DBDs. IM-MS was used in this study to separate species with different CCSs, including those with the same m/z but different overall mass and charge, and to characterize the number of DBDs in the different oligomers. The mobiligram of the SgrAI dimer−PC DNA complex at a molar ratio of 1:2 is shown in Figure 2. Peaks of SgrAI dimer−2PC DNA (1 × DBD), SgrAI tetramer−4PC DNA (2 × DBD) and SgrAI hexamer−6PC DNA (3 × DBD) complexes were observed in clusters I−III, respectively. A series of features were also observed in the boxed region of Figure 2B, in cluster VI, corresponding to the SgrAI dodecamer−12PC DNA (6 × DBD) complex. Because the intensities of these peaks are weaker than the intensities of the nonresolvable broad peaks in the range of m/z 9000−12000, they were not observed directly in Figure 1. IMS therefore facilitated the extraction of these "buried" peaks based on differences in drift time. The result shows the power of IMS to separate peaks of protein complexes or DNA−protein complexes having different drift times, even though these species have similar m/z values. Because clusters I−III

correspond to oligomers with 1 × DBD, 2 × DBD, and 3 × DBD, respectively, and cluster VI corresponds to oligomers with 6 × DBD, it follows that clusters IV and V would correspond to SgrAI−2PC DNA oligomers with 4 × DBD and 5 × DBD, respectively; however, no peaks in m/z could be resolved for confirmation. The inability to distinguish these directly may be due to the fact that larger species (i.e., larger than 6 × DBD) occur with m/z peaks similar to the peaks of 4 × DBD and 5 × DBD, or that neutral species binding to the complexes results in heterogeneity and m/z value overlap.

To identify the composition in clusters IV−V, the highest-intensity regions in these clusters in the 1:2.6 SgrAI dimer:PC DNA mobiligram were selected (Figures S4, S5, and S8 of the Supporting Information). SgrAI eicosamer−20PC DNA (10 × DBD) and SgrAI 38mer−38PC DNA (19 × DBD) complexes were observed in clusters IV and V of the mobiligram. The masses derived from the peaks agree well with the theoretical masses of SgrAI eicosamer−20PC DNA (10 × DBD) and SgrAI 38mer−38PC DNA (19 × DBD) complexes (Table S1 of the Supporting Information), and the observed peaks are reproducible (Figures S6 and S7 of the Supporting Information). The m/z peaks for these species are narrower than for the smaller oligomers because of region selection in IMS (see the text and Figures S9 and S10 of the Supporting Information). The discovery of large complexes, as well as the complexity of the spectrum hence requiring region selection, is consistent with the formation of a heterogeneous mixture of oligomers with different numbers of DBDs.[6] It is interesting that the total charge of these large species is approximately double that of globular proteins with similar masses.[60] This is likely due to a nonglobular shape of the SgrAI dimer−2PC DNA oligomers, because m/z is related to the surface area to volume ratio of the macromolecule.[60−62] It is possible that these were discerned only in the spectra with a higher ratio of PC DNA to SgrAI because of the formation of larger oligomers under these conditions. However, the diminished intensity in these regions with higher ratios of PC DNA to SgrAI suggests an effect of the DNA that reduces the amount of the larger oligomers, perhaps by competing with a second DNA binding site on SgrAI within the oligomer. Such a binding site is suggested by the dependence of oligomer formation on flanking DNA length.[6,10]

To further confirm the observation of SgrAI eicosamer−20PC DNA (10 × DBD) and SgrAI 38mer−38PC DNA (19 × DBD) complexes, their CCSs were compared with the CCSs of the smaller complexes. Figure 3 shows that the CCSs of the larger SgrAI−PC DNA complexes are on the same straight line as those of smaller SgrAI−PC DNA complexes. The CCSs suggest that the larger species observed have structures similar to those of smaller complexes. Further, the linear relationship suggests a regular, repeating structure, because each added DBD results in roughly the same increase in CCS. Because some oligomers differ by one DBD, this must be the basic building block of the oligomer. Both the regular, repeating nature of the structure and its heterogeneity in length are consistent with a run-on oligomer.

Model Building and CCS Calculations of SgrAI−DNA Complexes. The size of the 40-2 DNA or that of two PC DNA molecules annealed at the recognition sequence is 40 bp, approximately twice the size of two PC-9 DNA molecules [20 bp (Materials and Methods)]. However, the experimentally observed increase in CCS upon addition of PC-9 DNA to SgrAI dimer alone (black squares, Figure 4B) was much smaller than the increase in CCS upon addition of 40-2 DNA or two PC DNA molecules (each with 16 bp flanking each side of the recognition site) to the same (compare blue and purple triangles to red circles in Figure 4B). This is because the DNA inserts into the DNA binding site of SgrAI. To a first approximation, the overall size and shape of the SgrAI dimer are likely to be similar to those of the SgrAI dimer−2PC-9 DNA complex. When longer DNA is used, the flanking DNA is expected to extend away from the protein, consistent with the greater increase in the observed CCS.

The calculated CCS of the SgrAI dimer−2PC-9 DNA complex (blue dashed line, Figure 4B, and Table S6 of the Supporting Information) is close to (4% larger than) the experimental CCS determined for this complex (red circles, Figure 4B). The calculated CCSs of the three different models of the SgrAI dimer−2PC DNA complex are ∼62.0 nm^2 (1, red dashed line, Figure 4B), ∼60.0 nm^2 (2, red dashed line, Figure 4B), and ∼57.0 nm^2 (3, red dashed line, Figure 4B), which are 17, 13, and 7% larger, respectively, than the experimentally determined value for this complex (purple triangles, Figure 4B, and Table S6 of the Supporting Information). Therefore, the third conformation of flanking DNA for the SgrAI dimer−2PC DNA complex, with an 80° bend (3 of Figure 4A), is most consistent with the experimental CCS. The bend in DNA may be the result of the gas phase medium; with no solvent to shield the charge, the DNA bridges back to the protein.

The experimental CCS of the oligomer allows for comparison to possible models built from assemblies of the DBD. However, several different models were found to agree with the experimental CCS (data not shown). In addition, the likelihood of conformational changes that are expected to occur with activation of SgrAI in the oligomeric complex that are currently unknown adds further complexity to the modeling process. Therefore, a description of the SgrAI−DNA oligomer structure must await determination by higher-resolution structural methods, such as cryoelectron microscopy or X-ray crystallography. However, the CCS determined herein will provide an independent measure for comparison to any such model.

CONCLUSIONS

The masses of SgrAI−PC DNA complexes determined by IM-MS reveal that the basic building block of the SgrAI−DNA oligomer is the DBD with two copies of PC DNA per SgrAI dimer. The IM-MS data also show that this oligomer is heterogeneous and contains species with one to six DBDs, as well as some as large as 10 and 19 DBDs. This finding is similar to that previously reported using analytical ultracentrifugation.[11,51] Observation of the oligomers shows that nano-ESI-MS can preserve the noncovalent stoichiometries of both the native and activated forms of an enzyme. Finally, the CCSs of the oligomers of DBD show a linear relationship with the number of DBDs, showing that oligomers differing in the number of DBDs had similar changes in CCS and therefore a similar, regular structure.

Restriction endonucleases such as SgrAI are proposed to function as a defense against invading phage DNA. Cleavage of the host genome is prevented by methylation of SgrAI recognition sequences by the cognate SgrAI methyltransferase. SgrAI derives from *Streptomyces griseus*, a prokaryote with an unusually large genome (8.5 Mb, nearly twice the size of *Escherichia coli*). The relatively long (8 bp vs 4−6 bp) SgrAI recognition sequence may have evolved to reduce the number

of recognition sequences in the genome that would otherwise occur, which reduces the pressure in the form of sites required for methylation by the methyltransferase, as well as sites that could be potentially cleaved by SgrAI. Similarly, the relatively low DNA cleavage activity of unstimulated SgrAI may also have evolved to reduce this pressure. However, the low intrinsic cleavage activity and the reduced number of cleavage sites would both contribute to a less efficient defense against any invading phage DNA. Hence, the activation of SgrAI upon encounter of at least two unmethylated SgrAI recognition sequences, combined with the expansion of its sequence specificity, results in more cleavages occurring more rapidly to inactivate this invading DNA, but this activation and expansion of sequence specificity could in principle also harm the host genome. Therefore, the oligomerization of activated SgrAI may have evolved to sequester SgrAI on the phage DNA and away from the host genome.

■ ASSOCIATED CONTENT

Supporting Information

Spectra of SgrAI dimer−PC DNA complexes with different molar ratios, spectra with CID of SgrAI dimer:PC DNA molar ratios of 1:2.6 and 1:2, and tables containing the masses of SgrAI−DNA complexes, CID data, IM-MS CCSs of SgrAI−PC DNA complexes, and calculated CCSs of different SgrAI dimer−DNA complexes. This material is available free of charge via the Internet at http://pubs.acs.org.

■ AUTHOR INFORMATION

Corresponding Author

*V.H.W.: current address, Department of Chemistry and Biochemistry, The Ohio State University, Columbus, OH 43210; e-mail, wysocki.11@osu.edu; telephone, (614) 292-8687. N.C.H.: e-mail, nhorton@u.arizona.edu; telephone, (520) 626-3828.

Funding

This work was supported by National Science Foundation DBI Grant 0923551 to V.H.W.

Notes

The authors declare no competing financial interest.

■ ABBREVIATIONS

CCS, collision cross section; CID, collision-induced dissociation; DBD, DNA-bound SgrAI dimer; DTT, dithiothreitol; EHSS, exact hard sphere scattering; ENase, restriction endonucleases; IM-MS, ion mobility mass spectrometry; IMS, ion mobility spectrometry; MS, mass spectrometry; MS/MS, tandem mass spectrometry; nano-ESI, nanoelectrospray ionization; NMR, nuclear magnetic resonance; PA, projection approximation; PC DNA, precleaved SgrAI primary recognition site; PC-9, PC minus 9 flanking base pairs; TM, trajectory method; TOF, time-of-flight.

■ REFERENCES

(1) Bickle, T. A., and Kruger, D. H. (1993) Biology of DNA restriction. *Microbiol. Rev. 57*, 434−450.

(2) Kruger, D. H., and Bickle, T. A. (1983) Bacteriophage survival: Multiple mechanisms for avoiding the deoxyribonucleic acid restriction systems of their hosts. *Microbiol. Rev. 47*, 345−360.

(3) Boyer, H. W. (1971) DNA restriction and modification mechanisms in bacteria. *Annu. Rev. Microbiol. 25*, 153−176.

(4) McClelland, M. (1981) The effect of sequence specific DNA methylation on restriction endonuclease cleavage. *Nucleic Acids Res. 9*, 5859−5866.

(5) Bilcock, D. T., Daniels, L. E., Bath, A. J., and Halford, S. E. (1999) Reactions of type II restriction endonucleases with 8-base pair recognition sites. *J. Biol. Chem. 274*, 36379−36386.

(6) Park, C. K., Stiteler, A. P., Shah, S., Ghare, M. I., Bitinaite, J., and Horton, N. C. (2010) Activation of DNA cleavage by oligomerization of DNA-bound SgrAI. *Biochemistry 49*, 8818−8830.

(7) Tautz, N., Kaluza, K., Frey, B., Jarsch, M., Schmitz, G. G., and Kessler, C. (1990) SgrAI, a novel class-II restriction endonuclease from *Streptomyces griseus* recognizing the octanucleotide sequence 5′-CR/CCGGYG-3′ [corrected]. *Nucleic Acids Res. 18*, 3087.

(8) Bitinaite, J., and Schildkraut, I. (2002) Self-generated DNA termini relax the specificity of SgrAI restriction endonuclease. *Proc. Natl. Acad. Sci. U.S.A. 99*, 1164−1169.

(9) Hingorani-Varma, K., and Bitinaite, J. (2003) Kinetic analysis of the coordinated interaction of SgrAI restriction endonuclease with different DNA targets. *J. Biol. Chem. 278*, 40392−40399.

(10) Wood, K. M., Daniels, L. E., and Halford, S. E. (2005) Long-range communications between DNA sites by the dimeric restriction endonuclease SgrAI. *J. Mol. Biol. 350*, 240−253.

(11) Daniels, L. E., Wood, K. M., Scott, D. J., and Halford, S. E. (2003) Subunit assembly for DNA cleavage by restriction endonuclease SgrAI. *J. Mol. Biol. 327*, 579−591.

(12) Siksnys, V., Skirgaila, R., Sasnauskas, G., Urbanke, C., Cherny, D., Grazulis, S., and Huber, R. (1999) The Cfr10I restriction enzyme is functional as a tetramer. *J. Mol. Biol. 291*, 1105−1118.

(13) Deibert, M., Grazulis, S., Sasnauskas, G., Siksnys, V., and Huber, R. (2000) Structure of the tetrameric restriction endonuclease NgoMIV in complex with cleaved DNA. *Nat. Struct. Biol. 7*, 792−799.

(14) Vanamee, E. S., Viadiu, H., Kucera, R., Dorner, L., Picone, S., Schildkraut, I., and Aggarwal, A. K. (2005) A view of consecutive binding events from structures of tetrameric endonuclease SfiI bound to DNA. *EMBO J. 24*, 4198−4208.

(15) Nobbs, T. J., Szczelkun, M. D., Wentzell, L. M., and Halford, S. E. (1998) DNA excision by the Sfi I restriction endonuclease. *J. Mol. Biol. 281*, 419−432.

(16) Bozic, D., Grazulis, S., Siksnys, V., and Huber, R. (1996) Crystal structure of *Citrobacter freundii* restriction endonuclease Cfr10I at 2.15 Å resolution. *J. Mol. Biol. 255*, 176−186.

(17) Vipond, I. B., and Halford, S. E. (1995) Specific DNA recognition by EcoRV restriction endonuclease induced by calcium ions. *Biochemistry 34*, 1113−1119.

(18) Engler, L. E., Welch, K. K., and Jen-Jacobson, L. (1997) Specific binding by EcoRV endonuclease to its DNA recognition site GATATC. *J. Mol. Biol. 269*, 82−101.

(19) Martin, A. M., Horton, N. C., Lusetti, S., Reich, N. O., and Perona, J. J. (1999) Divalent metal dependence of site-specific DNA binding by EcoRV endonuclease. *Biochemistry 38*, 8430−8439.

(20) Reid, S. L., Parry, D., Liu, H. H., and Connolly, B. A. (2001) Binding and recognition of GATATC target sequences by the EcoRV restriction endonuclease: A study using fluorescent oligonucleotides and fluorescence polarization. *Biochemistry 40*, 2484−2494.

(21) Nastri, H. G., Evans, P. D., Walker, I. H., and Riggs, P. D. (1997) Catalytic and DNA binding properties of PvuII restriction endonuclease mutants. *J. Biol. Chem. 272*, 25761−25767.

(22) Etzkorn, C., and Horton, N. C. (2004) Ca^{2+} binding in the active site of HincII: Implications for the catalytic mechanism. *Biochemistry 43*, 13256−13270.

(23) Joshi, H. K., Etzkorn, C., Chatwell, L., Bitinaite, J., and Horton, N. C. (2006) Alteration of sequence specificity of the type II restriction endonuclease HincII through an indirect readout mechanism. *J. Biol. Chem. 281*, 23852−23869.

(24) Heck, A. J. (2008) Native mass spectrometry: A bridge between interactomics and structural biology. *Nat. Methods 5*, 927−933.

(25) Benesch, J. L., Ruotolo, B. T., Simmons, D. A., and Robinson, C. V. (2007) Protein complexes in the gas phase: Technology for structural genomics and proteomics. *Chem. Rev. 107*, 3544−3567.

(26) Hernandez, H., and Robinson, C. V. (2007) Determining the stoichiometry and interactions of macromolecular assemblies from mass spectrometry. *Nat. Protoc. 2*, 715−726.
(27) Veenstra, T. D. (1999) Electrospray ionization mass spectrometry: A promising new technique in the study of protein/DNA noncovalent complexes. *Biochem. Biophys. Res. Commun. 257*, 1−5.
(28) Loo, J. A. (1997) Studying noncovalent protein complexes by electrospray ionization mass spectrometry. *Mass Spectrom. Rev. 16*, 1−23.
(29) Rusconi, F., Guillonneau, F., and Praseuth, D. (2002) Contributions of mass spectrometry in the study of nucleic acid-binding proteins and of nucleic acid-protein interactions. *Mass Spectrom. Rev. 21*, 305−348.
(30) Pace, C. N., Trevino, S., Prabhakaran, E., and Scholtz, J. M. (2004) Protein structure, stability and solubility in water and other solvents. *Philos. Trans. R. Soc., B 359*, 1225−1234.
(31) Borsdorf, H., and Eiceman, G. A. (2006) Ion Mobility Spectrometry: Principles and Applications. *Appl. Spectrosc. Rev. 41*, 323−375.
(32) Borsdorf, H., Mayer, T., Zarejousheghani, M., and Eiceman, G. A. (2011) Recent Developments in Ion Mobility Spectrometry. *Appl. Spectrosc. Rev. 46*, 472−521.
(33) Shvartsburg, A. A., and Jarrold, M. F. (1996) An exact hard-spheres scattering model for the mobilities of polyatomic ions. *Chem. Phys. Lett. 261*, 86−91.
(34) Mesleh, M. F., Hunter, J. M., Shvartsburg, A. A., Schatz, G. C., and Jarrold, M. F. (1996) Structural information from ion mobility measurements: Effects of the long-range potential. *J. Phys. Chem. 100*, 16082−16086.
(35) Bush, M. F., Hall, Z., Giles, K., Hoyes, J., Robinson, C. V., and Ruotolo, B. T. (2010) Collision cross sections of proteins and their complexes: A calibration framework and database for gas-phase structural biology. *Anal. Chem. 82*, 9557−9565.
(36) Jurneczko, E., and Barran, P. E. (2011) How useful is ion mobility mass spectrometry for structural biology? The relationship between protein crystal structures and their collision cross sections in the gas phase. *Analyst 136*, 20−28.
(37) von Heiden, G., Hsu, M., Kemper, P. R., and Bowers, M. T. (1991) Structures of carbon cluster ions from 3 to 60 atoms: Linears to rings to fullerenes. *J. Chem. Phys. 95*, 3835−3837.
(38) Wyttenbach, T., von Helden, G., Batka, J. J., Carlat, J. D., and Bowers, M. T. (1996) Effect of the long-range potential on ion mobility measurements. *J. Am. Soc. Mass Spectrom. 8*, 275−282.
(39) Shvartsburg, A. A., Schatz, G. C., and Jarrold, M. F. (1998) Mobilities of carbon cluster ions: Critical importance of the molecular attractive potential. *J. Chem. Phys. 108*, 2416−2423.
(40) Ruotolo, B. T., Giles, K., Campuzano, I., Sandercock, A. M., Bateman, R. H., and Robinson, C. V. (2005) Evidence for macromolecular protein rings in the absence of bulk water. *Science 310*, 1658−1661.
(41) Ruotolo, B. T., Benesch, J. L., Sandercock, A. M., Hyung, S. J., and Robinson, C. V. (2008) Ion mobility-mass spectrometry analysis of large protein complexes. *Nat. Protoc. 3*, 1139−1152.
(42) Uetrecht, C., Barbu, I. M., Shoemaker, G. K., van Duijn, E., and Heck, A. J. (2011) Interrogating viral capsid assembly with ion mobility-mass spectrometry. *Nat. Chem. 3*, 126−132.
(43) van Duijn, E., Barendregt, A., Synowsky, S., Versluis, C., and Heck, A. J. (2009) Chaperonin complexes monitored by ion mobility mass spectrometry. *J. Am. Chem. Soc. 131*, 1452−1459.
(44) Knapman, T. W., Morton, V. L., Stonehouse, N. J., Stockley, P. G., and Ashcroft, A. E. (2010) Determining the topology of virus assembly intermediates using ion mobility spectrometry-mass spectrometry. *Rapid Commun. Mass Spectrom. 24*, 3033−3042.
(45) Politis, A., Park, A. Y., Hyung, S. J., Barsky, D., Ruotolo, B. T., and Robinson, C. V. (2010) Integrating ion mobility mass spectrometry with molecular modelling to determine the architecture of multiprotein complexes. *PLoS One 5*, 1−11.
(46) Hall, Z., Politis, A., Bush, M. F., Smith, L. J., and Robinson, C. V. (2012) Charge-state dependent compaction and dissociation of protein complexes: Insights from ion mobility and molecular dynamics. *J. Am. Chem. Soc. 134*, 3429−3438.
(47) Benesch, J. L., and Ruotolo, B. T. (2011) Mass spectrometry: Come of age for structural and dynamical biology. *Curr. Opin. Struct. Biol. 21*, 641−649.
(48) Scarff, C. A., Thalassinos, K., Hilton, G. R., and Scrivens, J. H. (2008) Travelling wave ion mobility mass spectrometry studies of protein structure: Biological significance and comparison with X-ray crystallography and nuclear magnetic resonance spectroscopy measurements. *Rapid Commun. Mass Spectrom. 22*, 3297−3304.
(49) Fernandez-Lima, F. A., Blase, R. C., and Russell, D. H. (2010) A study of ion-neutral collision cross section values for low charge states of peptides, proteins, and peptide/protein complexes. *Int. J. Mass Spectrom. 298*, 111−118.
(50) Dunten, P. W., Little, E. J., Gregory, M. T., Manohar, V. M., Dalton, M., Hough, D., Bitinaite, J., and Horton, N. C. (2008) The structure of SgrAI bound to DNA; recognition of an 8 base pair target. *Nucleic Acids Res. 36*, 5405−5416.
(51) Park, C. K., Joshi, H. K., Agrawal, A., Ghare, M. I., Little, E. J., Dunten, P. W., Bitinaite, J., and Horton, N. C. (2010) Domain swapping in allosteric modulation of DNA specificity. *PLoS Biol. 8*, e1000554.
(52) Cavaluzzi, M. J., and Borer, P. N. (2004) Revised UV extinction coefficients for nucleoside-5′-monophosphates and unpaired DNA and RNA. *Nucleic Acids Res. 32*, e13.
(53) Giles, K., Pringle, S. D., Worthington, K. R., Little, D., Wildgoose, J. L., and Bateman, R. H. (2004) Applications of a travelling wave-based radio-frequency-only stacked ring ion guide. *Rapid Commun. Mass Spectrom. 18*, 2401−2414.
(54) Shvartsburg, A. A., and Smith, R. D. (2008) Fundamentals of traveling wave ion mobility spectrometry. *Anal. Chem. 80*, 9689−9699.
(55) Giles, K., Williams, J. P., and Campuzano, I. (2011) Enhancements in travelling wave ion mobility resolution. *Rapid Commun. Mass Spectrom. 25*, 1559−1566.
(56) Zhou, M., Dagan, S., and Wysocki, V. H. (2012) Protein subunits released by surface collisions of noncovalent complexes: Nativelike compact structures revealed by ion mobility mass spectrometry. *Angew. Chem., Int. Ed. 51*, 4336−4339.
(57) DeLano, W. L. (2002) *The PyMOL User's Manual*, DeLano Scientific, Palo Alto, CA.
(58) Little, E. J., Dunten, P. W., Bitinaite, J., and Horton, N. C. (2011) New clues in the allosteric activation of DNA cleavage by SgrAI: Structures of SgrAI bound to cleaved primary-site DNA and uncleaved secondary-site DNA. *Acta Crystallogr. D67*, 67−74.
(59) Schooling, S. R., Hubley, A., and Beveridge, T. J. (2009) Interactions of DNA with biofilm-derived membrane vesicles. *J. Bacteriol. 191*, 4097−4102.
(60) Fernandez de la Mora, J. (2000) Electrospray ionization of large multiply charged species proceeds via Dole's charged residue mechanism. *Anal. Chim. Acta 406*, 93−104.
(61) Fernandez de la Mora, J. (2012) Why do GroEL ions exhibit two gas phase conformers? *J. Am. Soc. Mass Spectrom. 23*, 2115−2121.
(62) Kaltashov, I. A., and Mohimen, A. (2005) Estimates of protein surface areas in solution by electrospray ionization mass spectrometry. *Anal. Chem. 77*, 5370−5379.